LETTER

A Simple Design of Reconfigurable Intelligent Surface-Assisted Index Modulation: Generalized Reflected Phase Modulation

Chaorong ZHANG[†], **Yuyang PENG**[†a)], **Ming YUE**[†], *and* **Fawaz AL-HAZEMI**[††], ***Nonmembers***

SUMMARY As a potential member of next generation wireless communications, the reconfigurable intelligent surface (RIS) can control the reflected elements to adjust the phase of the transmitted signal with less energy consumption. A novel RIS-assisted index modulation scheme is proposed in this paper, which is named the generalized reflected phase modulation (GRPM). In the GRPM, the transmitted bits are mapped into the reflected phase combination which is conveyed through the reflected elements on the RIS, and detected by the maximum likelihood (ML) detector. The performance analysis of the GRPM with the ML detector is presented, in which the closed form expression of pairwise error probability is derived. The simulation results show the bit error rate (BER) performance of GRPM by comparing with various RIS-assisted index modulation schemes in the conditions of various spectral efficiency and number of antennas.
key words: *index modulation, GRPM, BER, spectral efficiency*

1. Introduction

In recent years, the reconfigurable intelligent surface (RIS) attracts plenty of attention in wireless communication area [1], [2]. As a potential member in beyond 5th generation (B5G) and 6th generation (6G) generation wireless communications, the RIS can be applied in many wireless-communication areas, e.g., index modulation, cooperative communication, non-orthogonal multiple access, etc. Compared with the traditional cooperative communication, the RIS, as a passive relay, needs less power to adjust the transmitted signal through the circuit unit on the RIS, which is named RIS controller. The RIS controller can make an adjustment of the reflected element to adjust the phase of the transmitted signal, which is called passive beamforming [3]. Some of the prior RIS researches consider the continuous phase adjusted at each reflected element, which is not practical and difficult to realize in real applications [4]. Due to this limitation in the RIS, the adjusted reflected phase needs to be discrete and quantized [5]. In this paper, an RIS-assisted index modulation scheme is designed with less discrete reflected phases, which can satisfy the requirement of hardware limitation and decrease the error detection caused by a greater number of discrete reflected phases.

After a few years researching and developing, index modulation has plenty of variants, e.g., the spatial modulation (SM), space shift keying (SSK), generalized space shift keying (GSSK), and so on. A larger number of prior works consider not only the antenna or antenna combination but also the active scatter [6] as index. With the popularity of the RIS application, the index modulation can be further developed by assisting with it. The reconfigurable intelligent surface-assisted space shift keying (RIS-SSK) is firstly proposed in [7], where the SSK works at the transmitter and the RIS is considered as a passive relay. In RIS-SSK scheme, the transmitter requires multiple transmitted antennas but only one can be used to transmit. Later, the intelligent reflecting surface-aided received GSSK scheme (IRS-RGSSK) is proposed in [8], where the received antenna combination is considered as the index and the RIS, as a passive relay, is divided into multiple parts to improve spectral efficiency. However, the IRS-RGSSK cannot ideally achieve the multiplexing merit for the bit error rate (BER), which indicates that the number of received antennas increase cannot bring the improvement of BER performance. The scheme of RIS-SSK modulation and reflection phase modulation (RPM) is proposed in [9], where the reflected phase is considered as the index and SSK is applied at transmitter. However, the scheme of RIS-SSK modulation and RPM [9] requires a greater number of transmitted antennas.

In order to improve the error performance and descend the number of transmitted antennas, a novel RIS-assisted index modulation scheme named as the generalized reflected phase modulation (GRPM) is proposed in this paper, where the proposed scheme combines the merits of the IRS-RGSSK [8] and reflection phase modulation (RPM) [9] schemes, i.e., the divided RIS reflected elements and the index of reflected phase. Besides, the GRPM not only can improve the multiplexing gain by increasing number of received antennas, but also achieve the same spectral efficiency with less number of transmitted antennas compared with the RPM scheme. The GRPM transmits unmodulated signal and the RIS adjusts the phase according to the reflected phase combination mapping table, which shows the corresponding relation between the conveyed bits and different reflected phase combination. The maximum likelihood (ML) detector is applied in the GRPM scheme, which is also presented with the theoretical analysis of pairwise error probability (PEP) in this paper. Eventually, the results show the better BER performance of the GRPM by comparing with the various RIS-assisted index modulation schemes, e.g., the IRS-RGSSK, RPM, and RIS-SSK, which demonstrates that the GRPM has more potential to be

Manuscript received March 2, 2023.
Manuscript revised April 26, 2023.
Manuscript publicized May 30, 2023.
[†]The authors are with the School of Computer Science and Engineering, Macau University of Science and Technology, Macau, China.
[††]The author is with Department of Computer and Network Engineering, University of Jeddah, Jeddah 21959, Saudi Arabia.
a) E-mail: yypeng@must.edu.mo (Corresponding author)
DOI: 10.1587/transfun.2023EAL2018

applied in real applications.

The rest of paper is organized as follows: In Sect. 2, the system model of the GRPM with ML detector is presented. The performance analysis of PEP in ML detector is presented in Sect. 3. The simulation results and conclusion of the GRPM and other RIS-assisted index modulation schemes are shown in Sect. 4. Finally, the paper conclusion is given in Sect. 5.

2. System Model

As shown in Fig. 1, the proposed scheme has a transmitter with one transmit antenna, a receiver with N_r receive antennas, and a RIS with N reflected elements. Specifically, the RIS is divided into z parts, where each part adjusts one specific reflected phase in each time slot and has $d = \lfloor \frac{N}{z} \rfloor$ reflected elements. The bit sequence is mapped into the index of reflected phase through the RIS controller. Then, according to the index, the RIS controller controls the reflected elements to adjust the phase of the transmitted signal φ_i into the mapped one, where $i = 1, 2, \ldots, N$. Some assumptions in the proposed scheme are given as follows:

- The channel fading h_i from the transmitter to the RIS and g_i from the RIS to the receiver are assumed to be Rayleigh flat fading [6]–[13].
- The direct link between the transmitter and the receiver is obstructed by a barrier. Besides, due to the reason that the power of received signal is proportional to the square of the number of reflected elements, the signal power from the direct link is much less than that from the RIS when N increases [9].
- The receiver has the perfect knowledge of channel state information (CSI) [7]–[13].
- The receiver is fixed in an appropriate place which is known by the RIS controller.

The reflected phases used for mapping the incoming bits can be adjusted in a given range, where each phase can be used for mapping the same bits. Among these available phases in the given range, the selection is dependent on the position of the receiver antenna. When the receiver moves to the next position, another phase in the given phase range will be selected to use for mapping the same bits but different receiver position. In other words, inside the phase range, all the phases can be used to express the incoming bits, but the difference of these phase is that they can be used to reflect the signal into different positions. According to the working principle of the proposed scheme, u discrete reflected phases are selected and divided to form the combinations to map into the incoming bits and adjusted through the reflected elements. Specifically, the reflected elements have z parts and each part has $\lfloor \frac{u}{z} \rfloor$ reflected phases to adjust, where the RIS can reflect the signal with z reflected phases to the receiver in each time slot. The multi-antenna diversity techniques can be applied at receiver to process the received signal [9]. This scheme can be applied in a practical scenario, where the receiver can be considered as a base station lied in a far field of the RIS and the transmitter is connected to the IRS controller [1]–[3]. Moreover, the whole scheme can be applied in a city, where plenty of buildings block the direct link between the transmitter and receiver, so the link through the RIS is the only way to reach the receiver. Besides, the bits mapped to the reflected phases can be generated based on the environment information which is collected by the sensors on or near the RIS. It is worth noting that the transmitted pure power signal can be extended to any M order quadrature amplitude modulation (QAM) or phase shift keying (PSK) modulated signal to further enhance the spectral efficiency, but this extension is not considered in this paper.

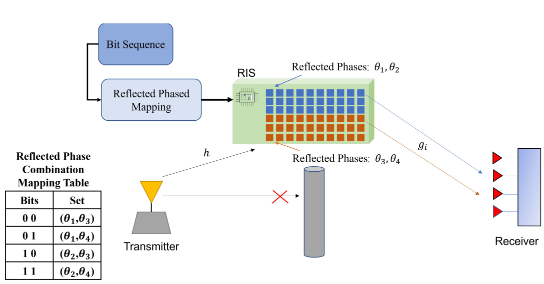

Fig. 1 System model of GRPM.

As for the reflected phases mapping, depending on the number of divisions in the reflected elements, the receiver can receive z reflected phases conveyed from the RIS. The z reflected phases can be constituted into an index combination $\boldsymbol{L}$, which is corresponding for different bits as shown in the mapping table in Fig. 1. Specifically, based on the example shown in Fig. 1, the reflected elements are separated into two parts, one of which has two different reflected phases, i.e., θ_1 and θ_2, or θ_3 and θ_4 to adjust. Thus, the reflected phases selected from various reflected elements parts are constituted an index combination, which is mapped into the bits. For instance, θ_1 and θ_3 are selected to indicate the bits (00).

In this regard, the total number of reflected phase combination is given by $b_t = \lfloor \frac{u}{2} \rfloor \binom{\lceil \frac{u}{2} \rceil}{1} = \lfloor \frac{u}{2} \rfloor^2$. Therefore, only $C_r = 2^{b_r}$ combinations can be selected, where b_r denotes the number of bits mapped to the reflected phase combination and is given by $b_r = \lfloor \log_2 b_t \rfloor$. Compared with the $b'_r = \lfloor \log_2 \mathrm{z} \rfloor$ in RPM, the transmitted number of phase-mapping bits in the GRPM dramatically increase especially when the u and z increase.

2.1 Transmission and Detection

The Rayleigh flat fading from the transmitter to the ith reflected element and from the ith reflected element to the receiver are respectively given as $h_i = \alpha_i e^{-j\omega_i}$ and $g_i = \beta_i e^{-j\varphi_i}$ following $\mathcal{CN}(0, 1)$ with zero mean and unit variance, where α and β represent the Rayleigh factors, and ω and φ respectively represent the unadjusted phases for the transmitted signal. For convenience, we define $H_i = \alpha_i \beta_i e^{-j(\omega_i + \varphi_i)}$. Thus, the received signal reflected by the ith reflected element can be given as:

$$y = \sqrt{E}\sum_{l=1}^{z}\sum_{i=(l-1)d+1}^{ld} H_i e^{j\phi_i^{\boldsymbol{L}\{l\}}} + n, \quad (1)$$

where E represents the unmodulated signal energy at receiver, n is the additive white Gaussian noise (AWGN) with zero mean and variance N_0, l represents the lth reflected phase in index combination, and $\phi_i^{\boldsymbol{L}\{l\}}$ is the adjusted phase selected in index combination $\boldsymbol{L}$ for the ith reflected element of the RIS. Furthermore, the signal-to-noise ratio (SNR) can be given as:

$$\mathrm{SNR} = \frac{E\left|\sum_{l=1}^{z}\sum_{i=(l-1)d+1}^{ld} H_i e^{j\phi_i^{\boldsymbol{L}\{l\}}}\right|^2}{N_0}. \quad (2)$$

Therefore, the maximum SNR can be given as:

$$\max\{\mathrm{SNR}\} = \frac{E\left|\sum_{l=1}^{z}\sum_{i=(l-1)d+1}^{ld} \alpha_i\beta_i\right|^2}{N_0}. \quad (3)$$

Assuming the CSI is perfectly known by the receiver, the ML detector is applied to detect the received signal, which can be given as:

$$\boldsymbol{P} = \underset{\boldsymbol{L}}{\operatorname{argmin}}\left\{\left|y - \sqrt{E}\sum_{q=1}^{z}\sum_{i=(q-1)d+1}^{qd}\alpha_i\beta_i e^{j\phi_i^{\boldsymbol{L}\{q\}}}\}\right|^2\right\}, \quad (4)$$

where $\boldsymbol{P}$ represents estimated reflected phase combination.

3. Performance Analysis

For the proposed scheme, the analytical BER performance of the divided elements design is estimated using the union bound technique. The average BER can be expressed as:

$$P_b \le E_{\boldsymbol{L}}\left[\sum_{q}\frac{D_H(\boldsymbol{L},\boldsymbol{P})\mathrm{P}(\boldsymbol{L}\to\boldsymbol{P}\mid H)}{2^{b_r}}\right], \quad (5)$$

where $E_{\boldsymbol{L}}[\cdot]$ represents the expectation operation, $D_H(\boldsymbol{L},\boldsymbol{P})$ represents the number of bits in error between $\boldsymbol{L}$ and $\boldsymbol{P}$, $\mathrm{P}(\boldsymbol{L}\to\boldsymbol{P}\mid H)$ represents the corresponding pairwise error probability (PEP). Thus, by defining $\lambda = \omega + \varphi$, the PEP can be expressed as:

$$\begin{aligned}&\mathrm{P}(\boldsymbol{L}\to\boldsymbol{P}\mid H)\\ &= \mathrm{P}\left\{\left(\left|y-\sqrt{E}H_{\boldsymbol{L}}\right|^2 - \left|y-\sqrt{E}H_{\boldsymbol{P}}\right|^2\right) > 0\right\}\\ &= \mathrm{P}\{-E\,|H_{\boldsymbol{L}}-H_{\boldsymbol{P}}|^2 - 2\sqrt{E}\Re\{(H_{\boldsymbol{L}}-H_{\boldsymbol{P}})n^*\} > 0\},\\ &= \mathrm{P}\{F > 0\}\end{aligned} \quad (6)$$

where

$$H_{\boldsymbol{L}} = \sum_{l=1}^{z}\sum_{i=(l-1)d+1}^{ld}\alpha_i\beta_i, \quad (7)$$

$$H_{\boldsymbol{P}} = \sum_{q=1}^{z}\sum_{i=(q-1)d+1}^{qd}\alpha_i\beta_i e^{j\left(\phi_i^{\boldsymbol{P}\{q\}}-\lambda_i\right)}, \quad (8)$$

with $\phi_i^{\boldsymbol{P}\{q\}}$ representing the adjusted phase selected in estimated index combination $\boldsymbol{P}$ for the ith reflected element, $\Re\{\cdot\}$ represents the real parts of a complex variable. Moreover, F is a complex Gaussian variable according to the principle of Gaussian distribution, which has the mean value $\mu_F = -\sqrt{E}|H_{\boldsymbol{L}} - H_{\boldsymbol{P}}|^2$ and variance $\sigma_F^2 = 2\sqrt{E}N_0|H_{\boldsymbol{L}} - H_{\boldsymbol{P}}|^2$. By applying the Q-function $Q(\cdot)$, the $\mathrm{P}(\boldsymbol{L}\to\boldsymbol{P}\mid H)$ can be extended as:

$$\mathrm{P}(\boldsymbol{L}\to\boldsymbol{P}\mid H) = Q\left(\frac{E\,|H_{\boldsymbol{L}}-H_{\boldsymbol{P}}|^2}{\sqrt{2N_0\,|H_{\boldsymbol{L}}-H_{\boldsymbol{P}}|^2}}\right). \quad (9)$$

Besides, by defining $D = H_{\boldsymbol{L}} - H_{\boldsymbol{P}}$ and applying the Central Limit Theorem when $N \gg 1$ [7], D follows the Gaussian distribution with the mean value $\mu_D = \frac{N\pi}{4}$ and variance $\sigma_D^2 = \frac{N(32-\pi^2)}{16}$. It is worth noting that $Var\{\alpha\beta\} = \frac{16-\pi^2}{16}$, $E\{\alpha\beta\} = \frac{\pi}{4}$, $Var\{H_{\boldsymbol{P}}\} = 1$, and $E\{H_{\boldsymbol{P}}\} = 0$.

By defining $\upsilon \triangleq |D|^2$, υ is a non-central chi-square distribution with one degree of freedom, and the PEP can be extended as:

$$\begin{aligned}\mathrm{P}(\boldsymbol{L}\to\boldsymbol{P}\mid H) &= \int_0^\infty Q\left(\sqrt{\frac{E\upsilon}{2N_0}}\right) f(\upsilon)\,d\upsilon\\ &= \frac{1}{\pi}\int_0^{\frac{\pi}{2}} M_\upsilon\left(-\frac{E}{4N_0\sin^2\eta}\right)d\eta,\end{aligned} \quad (10)$$

where we define $t = -\frac{\mathrm{E}}{4N_0\sin^2\eta}$ as the moment generating function of υ, with $M_\upsilon(t) = \left(\frac{1}{\sqrt{1-\sigma_D^2 t}}\right)\exp\left(\frac{\mu_D^2 t}{1-\sigma_D^2 t}\right)$ [8]. Furthermore, the upper bound of $M_\upsilon(t)$ can be obtained when $\sin^2\eta$ is equal to the maximum value 1, which can be expressed as:

$$M_\upsilon(t) \le \sqrt{\frac{64N_0}{64N_0 + E_sN(32-\pi^2)}}\,\mathrm{e}^{\left(\frac{-N^2\pi^2E}{64N_0+NE(32-\pi^2)}\right)}. \quad (11)$$

Thus, the upper bound of PEP can be expressed as:

$$\mathrm{P}(\boldsymbol{L}\to\boldsymbol{P}\mid H) \quad (12)$$

$$\le \frac{1}{2}\sqrt{\frac{64N_0}{64N_0 + E_sN(32-\pi^2)}}\,\mathrm{e}^{\left(\frac{-N^2\pi^2E}{64N_0+NE(32-\pi^2)}\right)}. \quad (13)$$

According to (12), since the variable N has square operation in $e^{(\cdot)}$, the PEP can be decreased by increasing N. Eventually, substituting (12) in (5), we can obtain the upper bound of average BER of the proposed scheme.

4. Simulation Results

In this section, the simulation results are shown and analyzed

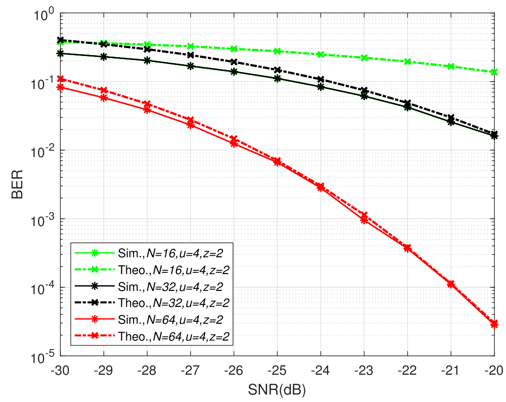

Fig. 2 Theoretical and simulation BER performance under various N of the GRPM.

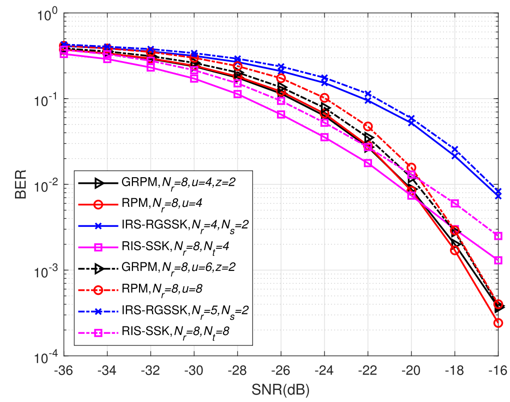

Fig. 4 Comparison of BER performance under various RIS-assisted index modulation schemes with different SE and N_r conditions.

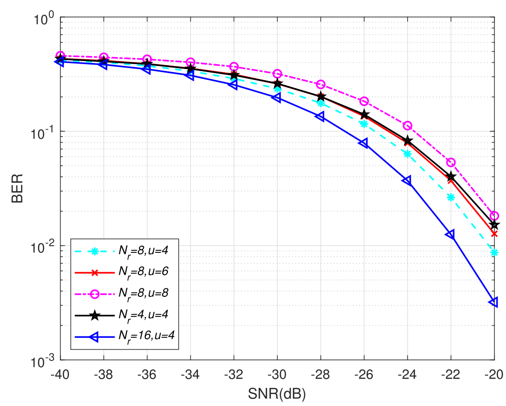

Fig. 3 Comparison of BER performance in various N_r and u conditions with $N = 32$ under the GRPM scheme.

to evaluate the performance and provide some conclusions of the proposed scheme. The comparisons among the different index modulation schemes are done under the same spectral efficiency (SE). The channel fading is assumed as Rayleigh flat fading and CSI is assumed to be perfectly known at receiver in all experimental results. To reduce the system complexity, the number of reflected phases z transmitted in each time slot is set to 2. Monte Carlo simulation is applied in the experiments running for 6×10^4 channel realizations.

Figure 2 shows the theoretical and simulation BER results of GRPM with $N = 16$, 32, and 64, where the SE is 2 bits/s/Hz by setting $u = 4$ and $z = 2$. In Fig. 2, the BER of GRPM decreases with the increase of N, especially when $N \gg 32$. Besides, the theoretical results get approached to the simulation ones with the increase of SNR and N.

In Fig. 3, the BER performance of the GRPM with $N = 32$, $N_r = 8$, and 16, as well as $u = 4$, 6, and 8 is shown. The scheme with $N_r = 8$ and $u = 4$ outperforms the one with $N_r = 4$ and $u = 4$, which concludes that BER performance gets better with the increase of N_r. The comparison of the scheme with $N_r = 8$, $u = 6$ under 3 bits/s/Hz and the scheme with $N_r = 4$, $u = 4$ under 2 bits/s/Hz shows that the BER performance of both almost coincide and the schemes with $N_r = 8$ show that the BER performance deteriorates with the increase of u.

The comparisons between various RIS-assisted index modulation schemes, i.e., GRPM, RPM, IRS-RGSSK, and RIS-SSK[†], are presented with various conditions in SE and N_r in Fig. 4. Firstly, under the same SE condition, the IRS-RGSSK has the worst BER performance compared with other RIS-assisted index modulation schemes due to the complexity and its BER increases with the increase of number of antennas at receiver [8]. On the contrary, the GRPM shows the better BER performance when N_r increases. As for the RIS-SSK, it shows better BER performance in low SNR situation, but worse BER performance in high SNR situation, i.e., SNR $\gg -20$ dB, compared with the GRPM and RPM. Secondly, the comparison between the GRPM and RPM shows that they have similar BER performance under the same SE condition, i.e., SE=2 bits/s/Hz and 3 bits/s/Hz. Specifically, by comparing with the BER performance of the RPM, Fig. 4 shows the BER of the GRPM is better under SE=3 bits/s/Hz when SNR $\ll -18$ dB and slightly better under SE=2 bits/s/Hz when SNR $\ll -20$ dB, due to the reason that the error performance of detection decreases with the increase of u in the low SNR situation. Because of the better BER performance in low SNR and high spectral efficiency conditions, the GRPM is a great choice in practical application.

5. Conclusion

By utilizing the characteristics of the RIS and index modulation, a novel RIS-assisted index modulation scheme named GRPM was proposed in this paper. Considering the constraint of the RIS hardware and better BER performance of the reflected phase detection, multiple reflected phases can be used as index and transmitted to the receiver in each time

[†]In the RPM, the elements are not divided into multiple parts, where only one phase as index can be used to convey the information to the receiver in each time slot [9]. For the RIS-SSK and IRS-RGSSK, they both apply the RIS to reflect the transmitted energy to the selected antenna or antennas at receiver [8], [10], where the receiver can obtain the transmitted bits by detecting the selected antenna or antennas.

slot. By applying the ML detector, a closed form expression of PEP over the Rayleigh flat fading channel was also presented in this paper to evaluate the upper bound expression of BER for the GRPM. Besides, the results show that the GRPM outperformed the other proposed RIS-assisted schemes, e.g., IRS-RGSSK and RIS-SSK, in the low SNR situation, e.g., IRS-RGSSK and RIS-SSK. In B5G and 6G wireless communication, high spectral efficiency and good BER performance are required. Thus, the GRPM has potential to satisfy the requirements and become a candidate of beyond 5G and 6G wireless commutations.

Acknowledgments

This work was supported in part by The Science and Technology Development Fund, Macau SAR (0108/2020/A3) and in part by The Science and Technology Development Fund, Macau SAR (0005/2021/ITP), in part by Wuyi University-Hong Kong-Macau joint Research and Development Fund (2021WGALH17).

References

[1] Q. Wu and R. Zhang, “Towards smart and reconfigurable environment: Intelligent reflecting surface aided wireless network,” IEEE Commun. Mag., vol.58, no.1, pp.106–112, 2020.

[2] Q. Wu and R. Zhang, “Intelligent reflecting surface enhanced wireless network: Joint active and passive beamforming design,” Proc. IEEE GLOBECOM, pp.1–6, 2018.

[3] M. Alsabah, M.A. Naser, B.M. Mahmmod, S.H. Abdulhussain, M.R. Eissa, A. Al-Baidhani, N.K. Noordin, S.M. Sait, K.A. Al-Utaibi, and F. Hashim, “6G wireless communications networks: A comprehensive survey,” IEEE Access, vol.9, pp.148191–148243, 2021.

[4] Q. Wu and R. Zhang, “Beamforming optimization for wireless network aided by intelligent reflecting surface with discrete phase shifts,” IEEE Trans. Commun., vol.68, no.3, pp.1838–1851, 2020.

[5] P. Xu, G. Chen, Z. Yang, and M.D. Renzo, “Reconfigurable intelligent surfaces-assisted communications with discrete phase shifts: How many quantization levels are required to achieve full diversity?,” IEEE Wireless Commun. Lett., vol.10, no.2, pp.358–362, 2021.

[6] Y. Ding, K.J. Kim, T. Koike-Akino, M. Pajovic, P. Wang, and P. Orlik, “Spatial scattering modulation for uplink millimeter-wave systems,” IEEE Commun. Lett., vol.21, no.7, pp.1493–1496, 2017.

[7] A.E. Canbilen, E. Basar, and S.S. Ikki, “Reconfigurable intelligent surface-assisted space shift keying,” IEEE Wireless Commun. Lett., vol.9, no.9, pp.1495–1499, 2020.

[8] C. Zhang, Y. Peng, J. Li, and F. Tong, “An IRS-aided GSSK scheme for wireless communication system,” IEEE Commun. Lett., vol.26, no.6, pp.1398–1402, 2022.

[9] U. Singh, M.R. Bhatnagar, and A. Bansal, “RIS-assisted SSK modulation: Reflection phase modulation and performance analysis,” IEEE Commun. Lett., vol.26, no.5, pp.1012–1016, 2022.

[10] E. Basar, “Reconfigurable intelligent surface-based index modulation: A new beyond MIMO paradigm for 6G,” IEEE Trans. Commun., vol.68, no.5, pp.3187–3196, 2020.

[11] S.P. Dash, R.K. Mallik, and N. Pandey, “Performance analysis of an index modulation-based receive diversity RIS-assisted wireless communication system,” IEEE Commun. Lett., vol.26, no.4, pp.768–772, 2022.

[12] S. Guo, J. Ye, P. Zhang, H. Zhang, and M.-S. Alouini, “Differential reflecting modulation for reconfigurable intelligent surface-based communications,” IEEE Commun. Lett., vol.25, no.3, pp.907–910, 2021.

[13] C. Zhang and Y. Peng, “Received antenna array design of GSSK-based antennas selection for RIS-assisted communication,” IEEE Syst. J., vol.17, no.2, pp.3366–3369, 2023. doi: 10.1109/JSYST.2022.3232998.